prepared for the
National Institutes of Health
National Institute of Neurological Disorders and Stroke
Neural Prosthesis Program
Bethesda, Maryland 20892

ELECTRODES FOR FUNCTIONAL ELECTRICAL STIMULATION

Contract #NO1-NS-6-2346

Quarterly Progress Report #3
May 1, 1997 - September 30, 1997

Principal Investigator
J. Thomas Mortimer, Ph.D.

Applied Neural Control Laboratory
Department of Biomedical Engineering
Case Western Reserve University
Cleveland, OH USA

TABLE OF CONTENTS

SECTION B. DESIGN AND FABRICATION OF ELECTRODES, LEADS AND CONNECTORS

B.2.1.1: Foil-Wigglewire-Foil (FWF) Cuff Electrodes

The foil-wigglewire-foil (FWF) electrode design described in our project proposal incorporates sinusoidally curving terminal lead wires that extend from a central coiled lead cable to platinum foil disks that serve as the contact sites. This design was developed to address the problem of excessive cuff stiffness that resulted when the terminal lead segments were straight wires. The sinusoidal shape of the terminal wires should allow for increased flexibility of the resulting electrode. This has been demonstrated in pilot laboratory studies.

The following figure is the schematic used in our contract proposal and describes the original idea for the FWF electrode. The terminal lead wires were to be configured in a sinusoidal pattern (WiggleWire Lead) that extended from the electrode contact to the lead cable.

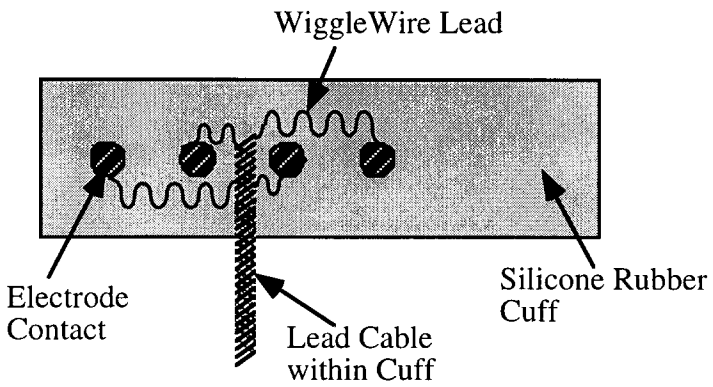

Figure 1: Schematic of the original FWF electrode design, as presented in the project proposal. Platinum foil disks that serve as the electrode contacts, are connected to a central coiled wire lead cable by sinusoidally curving terminal lead wires (WiggleWire Lead).

As we began to consider strategies for implementing this electrode, the possibility of using a laser machining approach was raised. Due to our initial success with laser machining for the PMP electrode (as discussed in the following section), we determined that the FWF design was very compatible with laser techniques and this would in fact, be simpler than conventional machining or metal forming methods.

Conceptually, the PMP and the FWF electrode designs we arrived at are very similar in nature, although the FWF electrode is a simpler pattern design than the detailed structure of the PMP. The same fabrication methods are incorporated into the proposed methodology for the FWF design as had been established for the PMP. First, a pattern is machined into a sheet of platinum foil. This pattern defines the basic electrical pathway and creates regions of stress relief within the substrate. This piece is laminated in silicone rubber that will provide structural support during the next phase of machining. This next phase involves a series of cuts that are strategically placed so as to electrically isolate the 4 electrode pathways. After these cuts, the perimeter of the piece is machined and a second lamination process follows that creates a spiraling cuff.

Electrode Design

To implement the FWF electrode using laser machining techniques, the basic design scheme of the proposed electrode was preserved. Modifications were included to increase the structural integrity of the substrate. The modified design is depicted in the figure below.

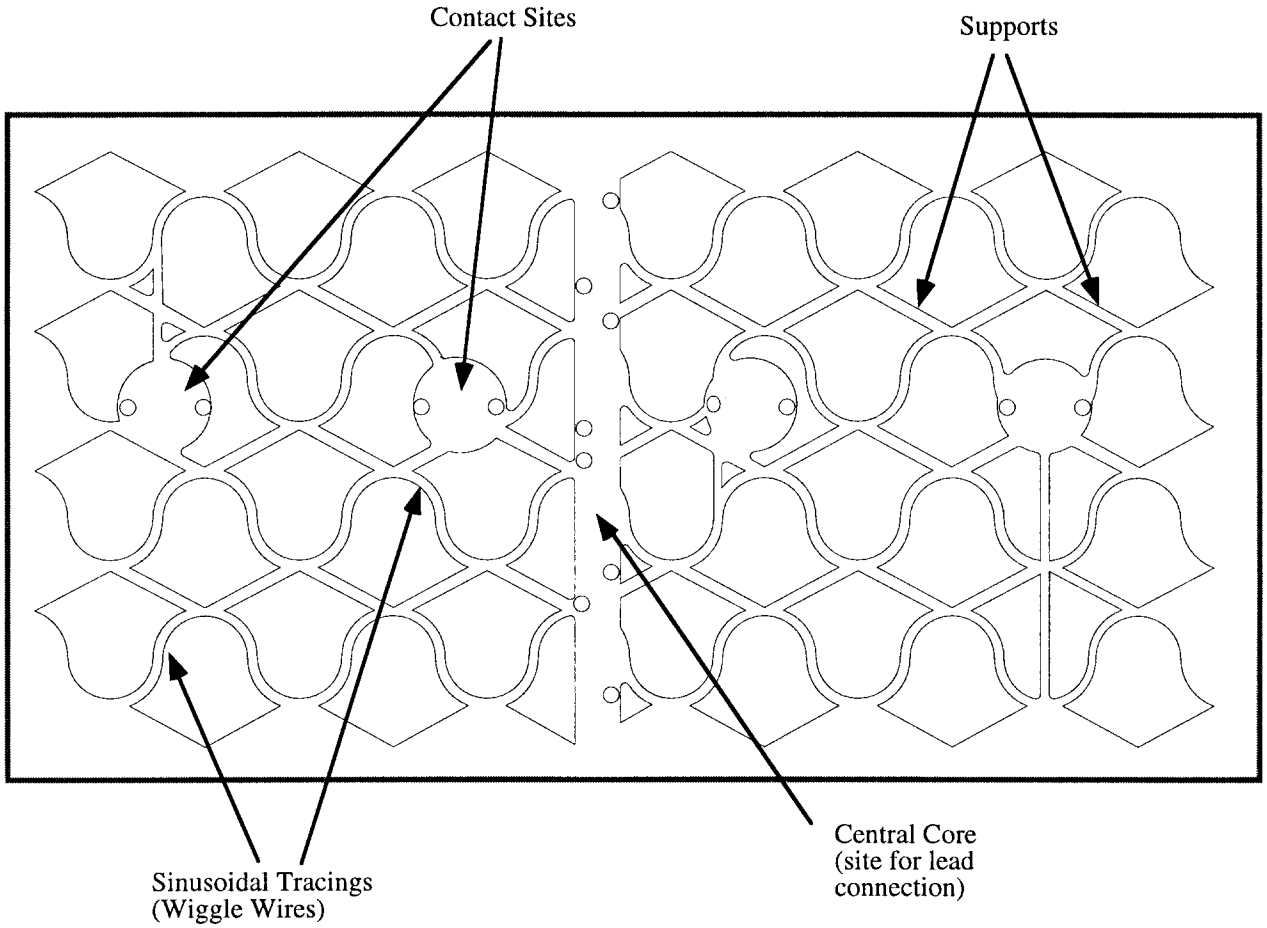

Figure 2: Schematic of the revised FWF electrode design that will be implemented using laser machining techniques. In this design, the central core, the electrode contacts, and the sinusoidal tracings are machined from a single piece of platinum foil. In the original design scheme, these elements would have been 3 separate pieces requiring welded connections.

A repeating pattern of sinusoidal traces covers the majority of the electrode piece. A central core provides the bonding sites for lead wire connection. Four, round contact sites are spaced along the length of the piece. Straight, short traces are left that lead from one sinusoidal trace to an adjacent trace. These are intended to provide mechanical support to the structure.

After the first pattern has been machined into the foil piece, the second step is to laminate the piece with silicone rubber. This lamination results in silicone rubber covering the top and bottom of the foil, as well as filling all the voids between the sinusoidal tracings.

Lamination is followed by a second pass of laser machining. This pass, as shown in Figure 3, is a series of arcs and circles (resembling hotdogs and hamburgers) that are spaced across the electrode piece. These cuts act to isolate each of the 4 electrode pathways. A third laser pass follows in which the final perimeter of the electrode piece is machined and the piece drops out (Figure 4).

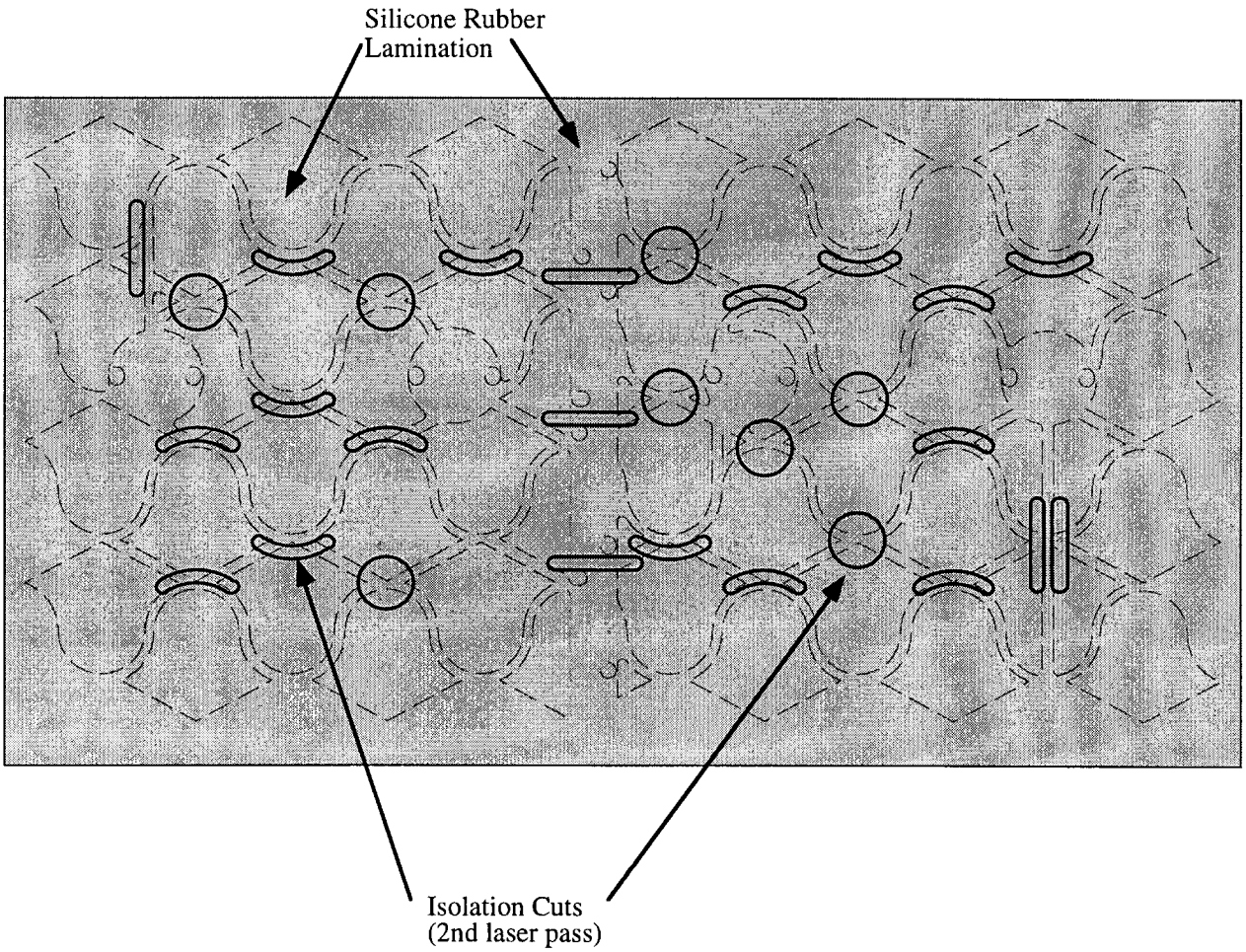

Figure 3: Schematic of the second pass of laser cuts in the FWF electrode design. These cuts, which are shaped like circles and arcs, are spaced so as to electrically isolate each of the 4 pathways. The cuts are made through the entire laminated structure, including the top and bottom layers of silicone rubber and the platinum foil in the center.

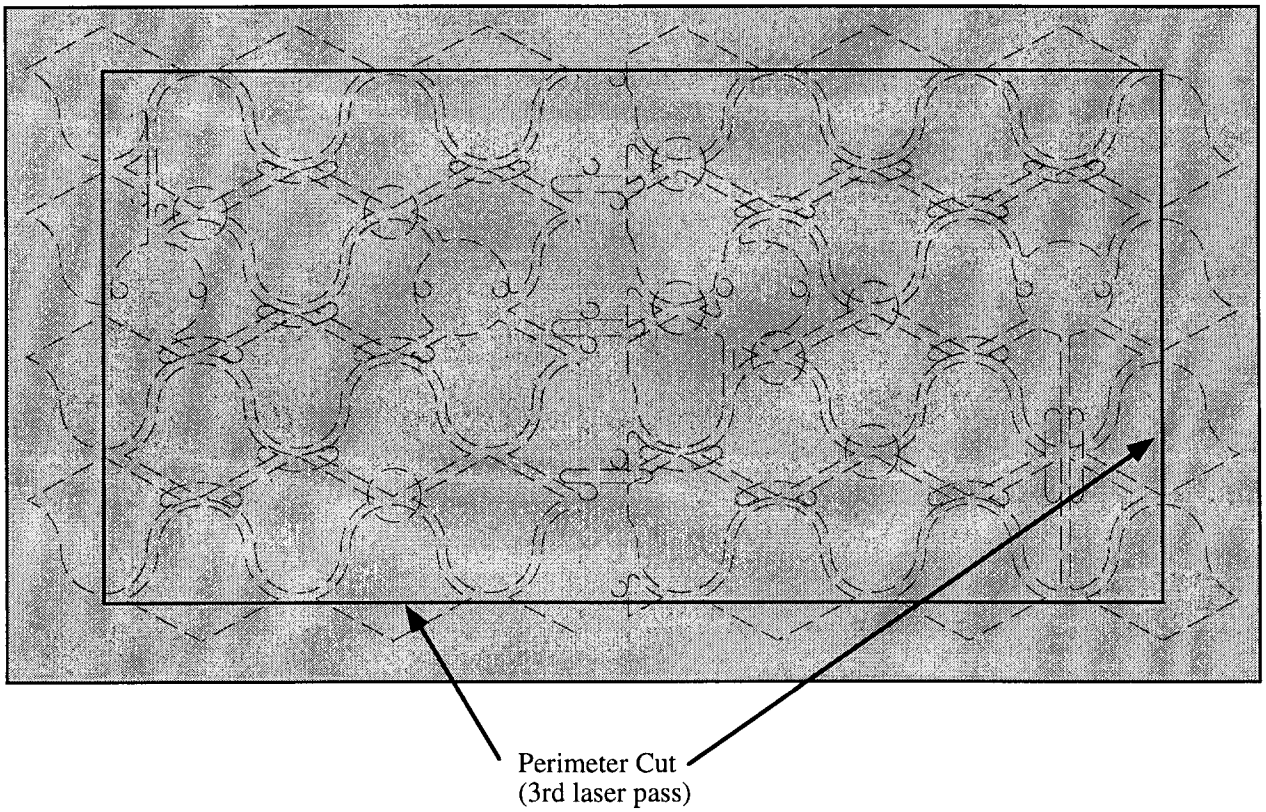

Figure 4: Schematic of the third pass of laser cuts in the FWF electrode design. This cut defines the perimeter of the electrode piece and acts to further electrically isolate the pathways. After this cut is machined, the piece drops out of the frame.

The second pass of laser cuts is followed by a final lamination that results in the spiral cuff. The lead wires are bonded on the back side of the spiral, creating an exterior backbone along the width of the cuff. The contact sites are exposed on the inside.

CAD File

Precision drawings of the electrode design were prepared in AutoCAD by an undergraduate student in our laboratory. The electrode design was separated into 3 layers: the initial pattern, the isolation cuts, and the perimeter cuts. These drawings are shown in the preceding figures, Figures 2-4.

Production of Prototype

Our experience with the PMP electrode suggested that a 50μm foil thickness should provide adequate flexibility for spiral cuffs. We therefore limited our initial production of the FWF electrode to only the 50μm foil, and did not investigate the 25μm foil. A frame with the appropriate inner dimensions for the FWF design was constructed to secure the foil during the machining steps.

Step 1: First Laser Pass

The initial fabrication step was performed and involved the machining of the basic pattern in the platinum foil. This step was performed without complication and the piece was examined prior to subsequent fabrication steps.

The patterned foil was examined with light and scanning electron microscopy. Similar edge roughness was noted as had been observed with the PMP prototype. The pattern appeared to match the specifications of the drawing. Photomicrographs of the prototype are presented in Figures 5-9.

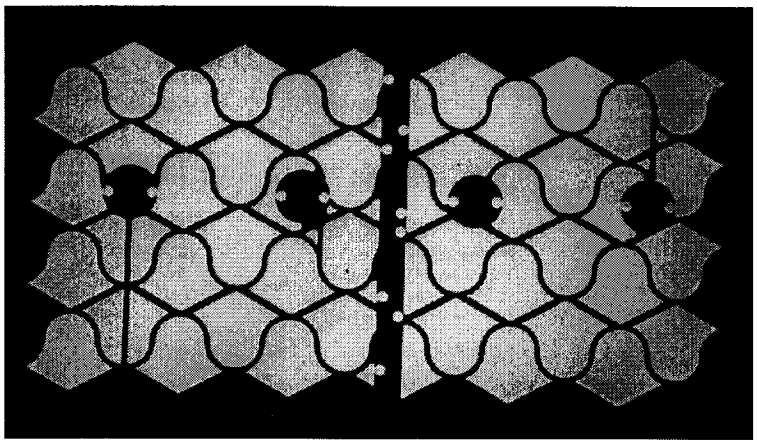

Figure 5: Photograph of FWF prototype after the first pass of laser machining. The platinum foil is the darkened structure in the photo and the light regions are where pieces of the foil piece have been machined out.

A. 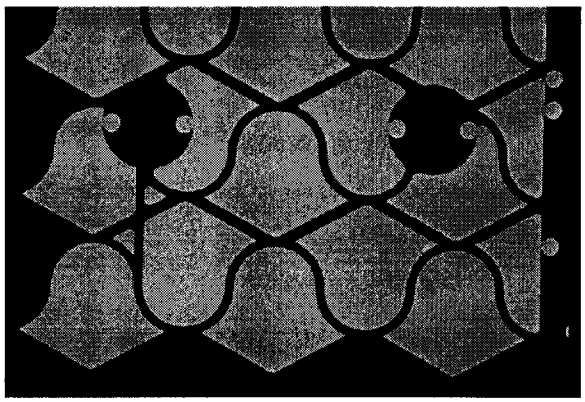

B. 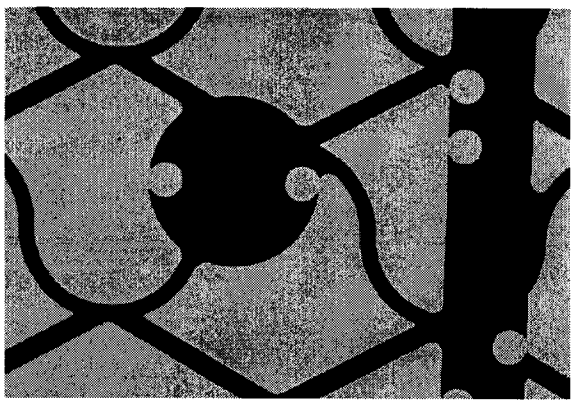

Figure 6: Higher magnification photos of the FWF prototype after the first pass of laser machining. The repeating bell-shaped pattern that defines the sinusoidal tracings and the straight support segments is seen in view A. Details of an individual trace and a contact pad are shown in view B. The small circular openings at the edges of the contact pad and along the edges of the center core are designed to provide further securing of the foil by the silicone rubber.

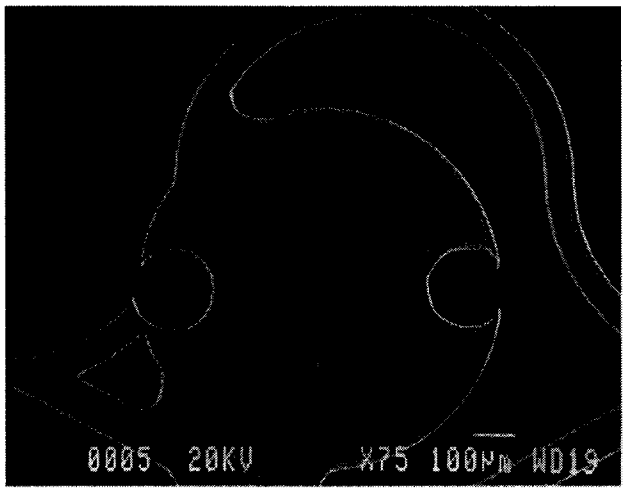

Figure 7: SEM photomicrograph of the FWF prototype after the first pass of laser machining. A contact pad is shown in the photo.

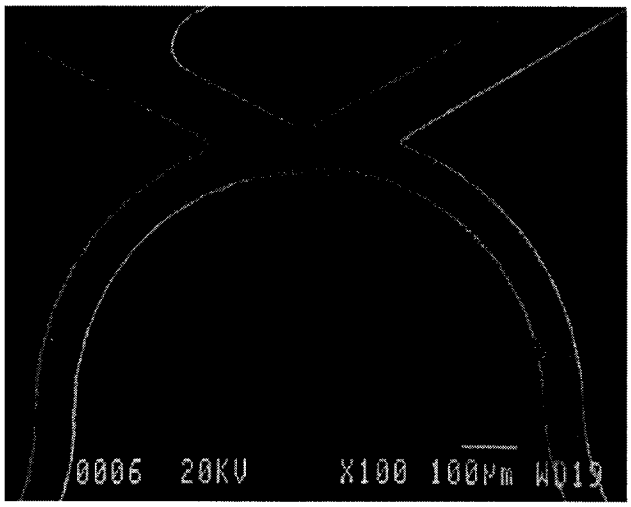

Figure 8: SEM photomicrograph at higher magnification, showing detail of the sinusoidal tracing and straight support segments.

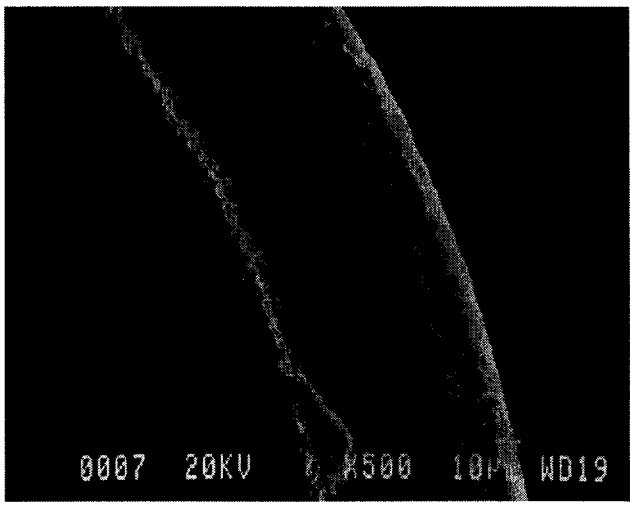

Figure 9: SEM photomicrograph at higher magnification, showing details and edge condition of the sinusoidal tracing in Figure 8. The edge roughness is similar to what was found with the PMP prototype.

Step 2: Lamination of Foil

After examination, the piece was laminated following our standard methods. The foil and a small volume of silicone rubber elastomer were sandwiched between two unstretched sheets of 50μm thick silicone rubber sheeting. This assembly was placed between 2 plates and put in a laboratory press. The final laminated thickness was set to the minimum of 150μm (top sheet + foil + bottom sheet). When the plates were opened and the laminated piece removed, a small wrinkle on the back side of the foil was observed. As shown in Figure 10, this wrinkle was visible upon close examination, but did not appear to be of significant height dimension. We determined that the wrinkle, because it was located on the back side, seemed unlikely to cause significant lasing or location problems.

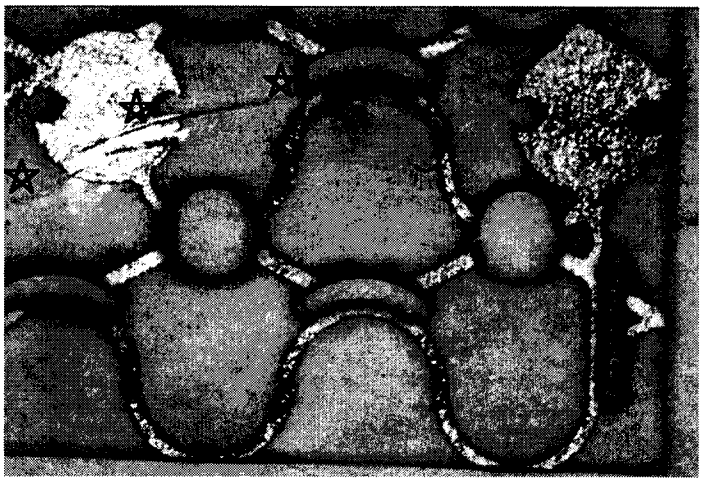

Figure 10: Photograph of the FWF prototype after the silicone rubber lamination. A wrinkle is seen extending from the center left edge, across the left most contact pad, into the adjacent sinusoid tracing. A series of *s marks the path of the wrinkle.

Step 3: Second Laser Pass

The second pass of laser cuts was performed and the perimeter was cut. The FWF electrode was examined with light microscopy before proceeding with the final lamination. The arc cuts appeared to be slightly overlapping the sinusoid tracings, actually cutting the 'wire' trace. These arc cuts were meant to remove silicone rubber and the metal supports adjacent to the tracings without compromising the sinusoidal shape. Additionally, we noted that electrical continuity had been preserved between several electrode pathways that were intended to be isolated from one another. The drawings were in error and some cuts had inadvertently been omitted from the final design figures. We proceeded with the fabrication steps, knowing that while the electrical isolation between the 4 pathways could not be tested, the overall flexibility and concept of the FWF design could be evaluated once the prototype was formed into a cuff.

Step 4: Lamination to Make Spiral Cuff

As was done with the PMP prototype, we followed standard methods for production of a spiral cuff. A thin layer of uncured silicone elastomer was first spread in the center of the bottom plate. The FWF piece was laid on this and additional elastomer was spread to cover the electrode piece. A 75μm thick silicone rubber sheeting was used for the top, stretched layer, with the degree of stretch calculated according to our standard formula for a 3mm diameter cuff. Without having prior experience in spiraling the FWF substrate, we felt this was a best-guess starting point. The stretched layer was placed over the electrode and any visible air bubbles in the elastomer were

forced to the side using a soft-tipped probe. The sheeting backing, a Mylar-type material, was placed on top of the stretched sheet. Shim stock was positioned at the edge of the plate to define the final thickness and the top plate was gently set in place. This assembly was then put in the laboratory press.

After an hour at elevated temperature and pressure, the assembly was removed from the press and allowed to cool. The plates were opened and the general cuff shape was cut from the surrounding silicone rubber. The final cuff is flexible and spirals to an approximate inner diameter of 3-4 mm. Visual and microscopic examination of the electrode showed that some areas of the foil electrode had mechanically deformed. Distortion of the sinusoidal curves could be noted in regions and displacement and breakage of some of the support spans was seen in other areas. Neither of these resulted in breakage of the electrical pathways. The general appearance and feel of the FWF spiral cuff was very consistent with our expectations and past experience with spiral cuffs.

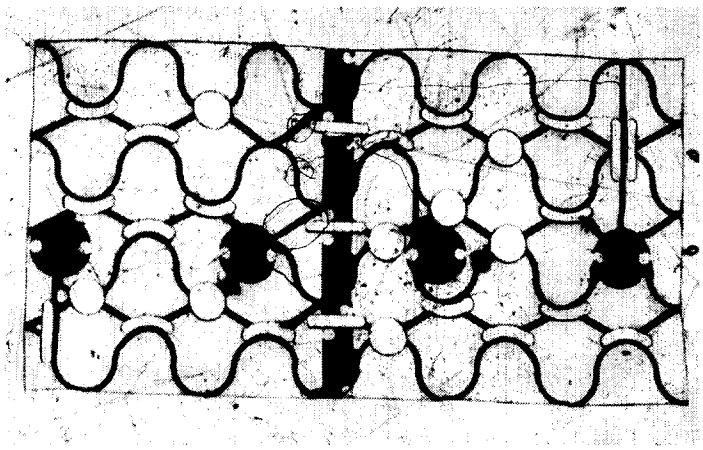

Figure 11: Photograph of the FWF electrode prototype. A faint line can be noted that defines the border created during the third laser pass. Some distortion of the sinusoidal traces can be seen. Particulate matter adhering to the silicone rubber surface is apparent on the entire piece.

A. 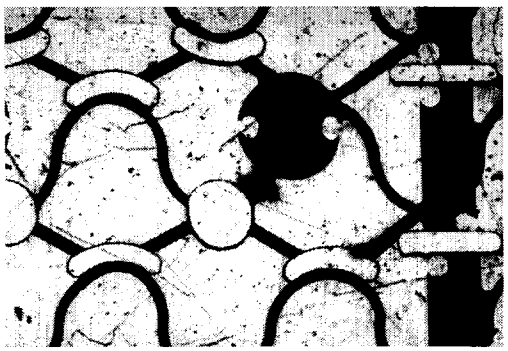 B. 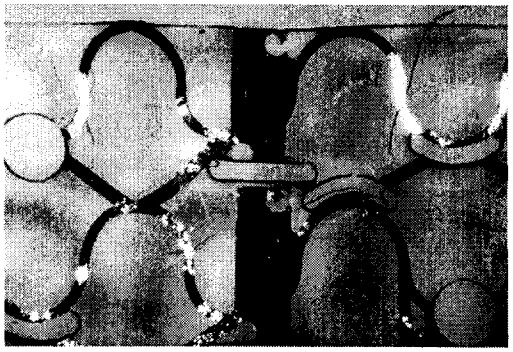

Figure 12: Higher magnification photographs of the FWF prototype. Distortion in the tracings, as well as distortion of the isolation cuts from perfect circles and arcs is apparent. In view A, a blurry region located just below the contact pad may be indicative of a metal break. Although some glare is present in view B, a break in one of the sinusoidal tracings is clearly seen.

Future Work

Although the FWF electrode design is simpler to machine than the PMP electrode, we are not as confident in this electrode's mechanical reliability. In comparing the two designs, we feel that the ratio of silicone rubber to platinum in the FWF electrode is probably too high. Not enough platinum is left within the substrate to hold the structure in place when the final spiral cuff is formed. Distortion and breakage of the platinum foil tracings are indicators of this. Beyond the distortion that was evident in the design, the final cuff does not qualitatively feel as flexible or robust as the PMP.

Our experience with the FWF electrode has led us to conclude that the sinusoidal wiggle is flexible enough to allow the cuff to spiral. However, the relatively small amount of metal compared to the volume of silicone rubber and the long wavelength of the design results in some distortion and questionable mechanical stability. We intend to incorporate some of the features of the FWF design into a revised PMP electrode scheme that we think will optimize the mechanical reliability and flexibility of the final electrode piece.

SECTION B. DESIGN AND FABRICATION OF ELECTRODES, LEADS AND CONNECTORS

B.2.1.2: Polymer-Metal Foil-Polymer (PMP) Cuff Electrodes

The polymer-metal foil-polymer (PMP) electrode is a novel design that attempts to improve the mechanical reliability and ease the manufacturing process of spiral nerve cuff electrodes. The electrode design relies upon laser micromachining technology applied to both metal foils and polymer-metal foil laminates. A prototype cuff has been fabricated and the results prove the feasibility of the concept. Minor changes to the design specifications and the fabrication protocols are warranted to improve the final outcome and will be pursued in coming months.

Previous Work

Step 1: First Laser Pass

The initial step in fabricating the PMP electrode is the first pass of laser cuts that create the pattern of holes throughout the platinum foil piece. This pass of laser cuts was performed to begin production of a prototype in both 25 and 50μm foil. The foil pieces were examined using light and scanning electron microscopy. The quality and dimensions of the laser cuts appeared to be adequate and we proceeded with the fabrication of the prototypes.

Current Work

Step 2: Lamination of Foil

After the first pass of laser cuts were made, the next step was to laminate the foil in silicone rubber. Our intention was to follow the general procedure we use to make a spiral cuff: sandwiching uncured silicone elastomer and the platinum foil between 2 layers of pre-formed silicone rubber sheeting. For the lamination, the top layer of silicone rubber sheeting is not stretched, as we do not want the laminated piece to form a self-wrapping spiral. Our primary concerns about this approach were (1) how well the uncured elastomer would spread to fill all of the voids in the platinum foil, and (2) how well we would be able to produce an even thickness coating over the platinum foil.

Sample Laminations

Before performing the lamination on the prototypes, sample pieces of foil were laminated to test the feasibility of this approach. Pieces of foil, both 25 and 50μm thick, on which practice laser machining had been performed were used. The attempts at lamination were largely successful and we determined that using mold release on the plates in combination with leaving the backing on the sheeting greatly aided in removal of the laminated foil from between the plates. However, even with these accommodations, the laminated foil was difficult to remove from one side of the backing, particularly in the case of the 25μm foil. Often, the adhesion was so great that the foil had to be mechanically deformed and bent to remove it from the backing, leaving a crease in the foil.

Prototype Laminations

Despite this complication, we proceeded with the lamination of the prototypes in the interests of time. The prototype foil was sandwiched between 2 unstretched layers of 50μm silicone rubber sheeting and silicone rubber elastomer. For the 50μm foil, the final thickness was set to 150μm; for the 25μm foil, the final thickness was set to 125μm. In both cases, the foil did adhere to the backing material and special effort had to be made to remove the laminated structure. Minimal deformation was required for the 50μm foil; the slight creases that resulted were located at the edge of the foil piece, away from the machined area. The 25μm foil was much more strongly adhered and increased efforts were expended to remove the backing. In the process, multiple creases and wrinkles were created in the foil, including throughout the machined area.

In considering this problem, it would appear that the silicone rubber is very well adhered to the backing after having been in the press. This is exacerbated at the site of the foil piece, as there is additional bulk of material that can be pressed into the backing. To remove the backing, it can be bent in small increments and this bend will act to pull the 2 layers apart. In the case of the 50μm foil, the inherent stiffness of the foil is great enough to pull the layers apart. However, the 25μm foil is not stiff enough to overcome the adhesive forces. When the backing is bent, the 25μm foil bends with the backing, rather than pulling away. Immersion of the piece in solution and application of alcohol did not aid in removal of the laminated structure. To avoid this complication in the future, we may try to use the mold release agent not just on the plates, but directly between the backing and the sheeting.

Because of the damage done to the 25μm prototype, we decided to proceed with the additional fabrication steps of the 50μm foil only. Based on the results we would obtain with the 50μm foil, we would decide whether pursuing the 25μm foil further was warranted.

Step 3: Second Laser Pass

In this step, cuts are made through both the silicone rubber and platinum foil to isolate each electrical pathway. Then, the outer perimeter is cut, dropping the PMP structure out of the surrounding foil and silicone rubber.

Sample Machining

Sample laminated foils were prepared to be used for practice machining and establishment of lasing parameters. Pieces of foil, measuring approximately 1cm by 2cm were laminated using a top layer of unstretched NuSil sheeting, and a middle layer of uncured elastomer. The bottom layer was either NuSil or Silablate sheeting. A total of 4 samples were prepared: 25μm foil with NuSil-Silablate sheeting, 25μm foil with NuSil-NuSil sheeting, 50μm foil with NuSil-Silablate sheeting, and 50μm foil with NuSil-NuSil sheeting. Although we had already decided to use only NuSil materials for our prototype lamination, we were curious to see the difference between the machined NuSil and the machined Silablate.

Light and scanning electron microscopic examination of the sample machining was performed and photomicrographs are presented below. Although the Silablate material appears to have machined with cleaner features than the NuSil product, the apparent differences are minimal. In either case, the features are easily within our specifications for the PMP electrode. Based on these observations and our previous concerns about the strength of Silablate materials, we are comfortable proceeding with the NuSil products in our development of the PMP electrode.

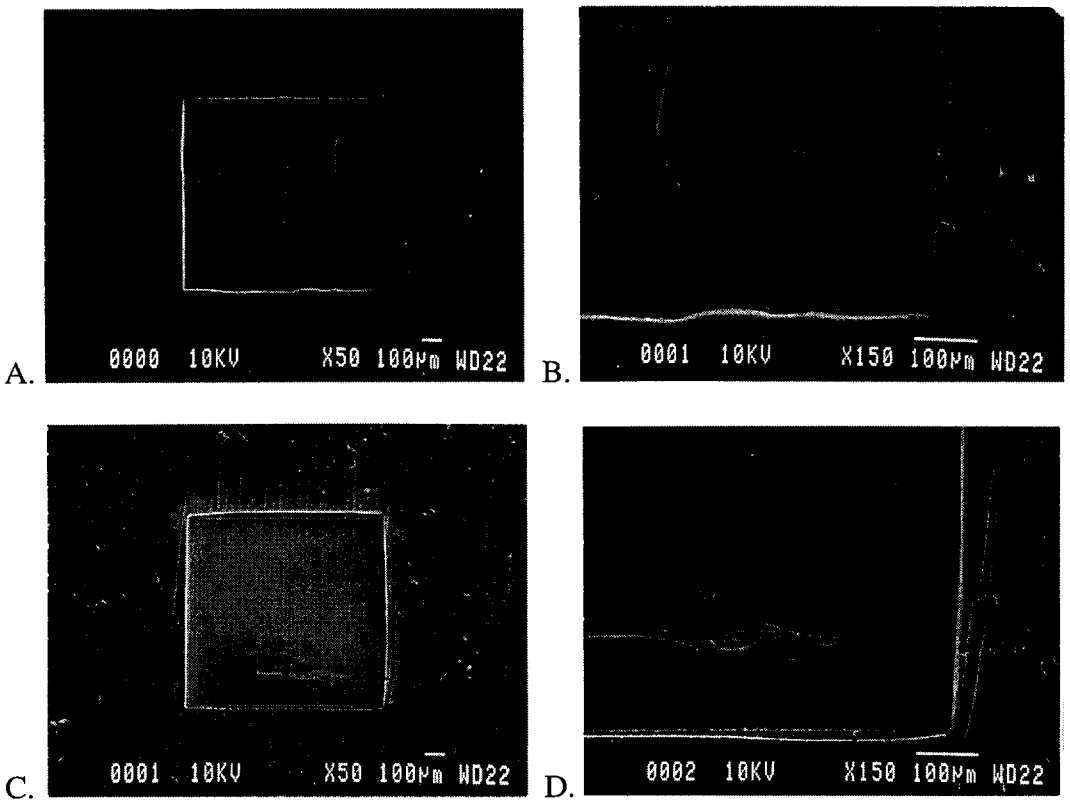

Figure 13: SEM photomicrographs of 50µm foil laminated in silicone rubber. Practice laser machining was performed to remove only the top layer of silicone rubber. The sample in the top photos (views A and B) was laminated in NuSil silicone rubber sheeting, while the sample in the lower photos (views C and D) was laminated with Silablate silicone rubber sheeting. High magnification views of the lower right corner of the cut in A and C are shown in B and D, respectively.

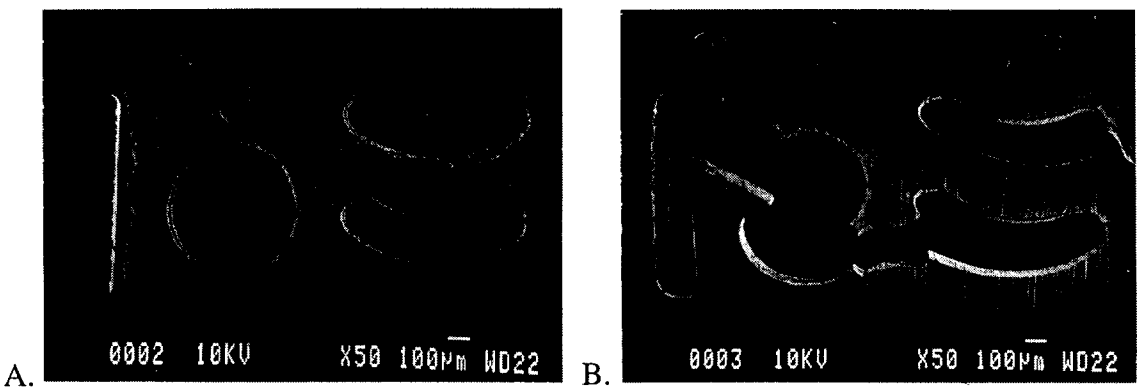

Figure 14: SEM photomicrographs of 50µm foil laminated in silicone rubber. Practice laser machining was performed to cut entirely through the laminated structure. The shape of the cuts resemble those of the 2nd pass (isolation cuts) for the FWF design. The sample in A was laminated with NuSil silicone rubber sheeting, while the sample in B was laminated with Silablate silicone rubber sheeting. In preparing sample B for SEM evaluation, the silicone rubber was

accidentally pulled, resulting in some tears and separation of the lamination from the underlying platinum foil.

Prototype Machining

The second pass of laser cuts, those that isolate the electrical pathways, were machined first. Then, the third laser pass was made that cuts out the final perimeter of the PMP. This cut separates the electrode from the exterior foil, further isolating the pathways, and the piece essentially drops out of the frame. This final piece was placed between 2 glass slides.

We examined the prototype using a light microscope without removing the piece from between the slides. Discoloration caused by the laser was noted around many of the cuts; the silicone rubber was darkened, making it difficult to distinguish between the silicone rubber and the platinum. Although it appeared that the second pass of cuts did effectively isolate each pathway, we were concerned that these cuts penetrated too deeply into the silicone rubber islands. Only a very narrow span of silicone rubber was left between the metal tracings. Our concern was that this small amount of material would not provide sufficient strength to hold the assembly together during the lamination.

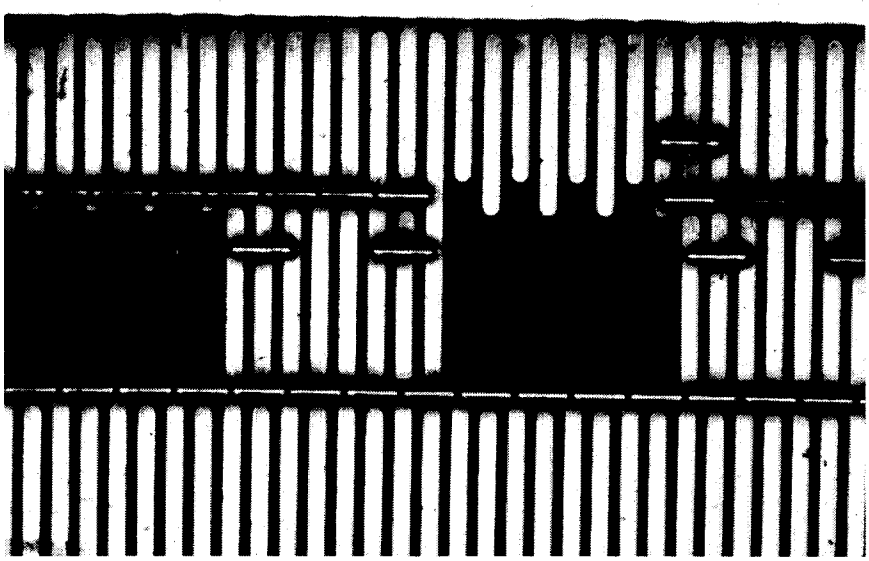

Figure 15: Photograph of the PMP prototype after the 2nd pass of laser machining. Discoloration of the silicone rubber at the edges of the cuts make it difficult to distinguish the boundary between the silicone rubber and the platinum foil. Only very narrow spans of silicone rubber are left between adjacent 'rows' that define the electrical pathways. The basic structure of the electrode design has maintained its integrity and the placement of the isolation cuts appear to be accurately aligned.

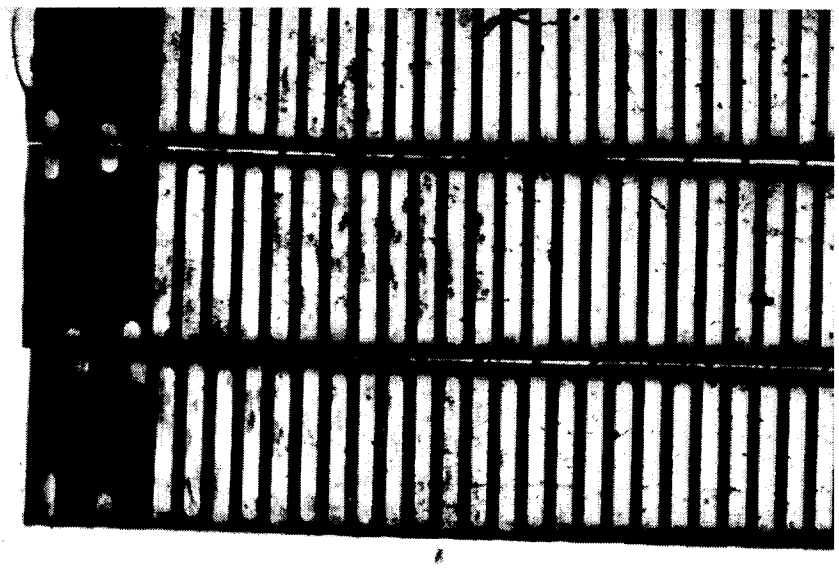

Figure 16: Photograph of the PMP prototype after opening the glass slides. Although it is difficult to distinguish, the silicone rubber spans holding the lower path in alignment with the rest of the electrode, have torn for a short distance from the edge inward. Adhesion between the electrode substrate and the glass slides caused the electrode to tear as the slides were separated.

The glass slides were opened to expose the foil piece for further examination and cleaning. As the slides were separated, the silicone rubber adhered to both slides, and a portion of the electrode pulled apart at one end. When examined microscopically, some of the silicone rubber islands between 2 adjacent pathways had torn. These tears were located at the far end of the electrode, and can be seen in Figure 16. The piece then had to be removed from the glass slide for cleaning before the final lamination. In removing the electrode from the slide, significant adhesive forces were noted. Sonication in surfactant and alcohol solutions did not overcome this adhesion. A fine forcep to pry up the piece, in combination with an alcohol rinse, were used to forcibly remove the electrode. In the process, additional islands of silicone rubber were broken and some foil traces were distorted. A photograph of the PMP demonstrating some of this damage is presented in Figure 17.

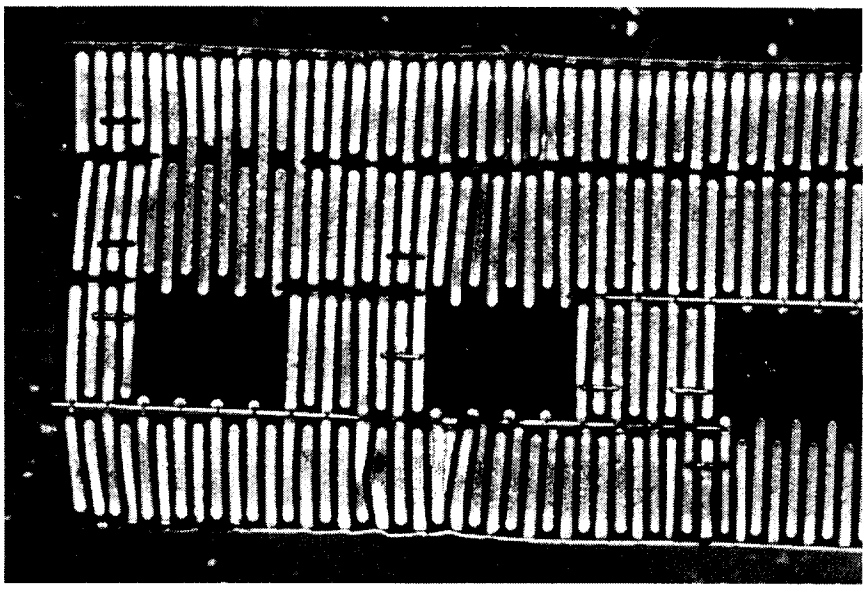

Figure 17: Photograph of the PMP prototype after it had been forcibly removed from the glass slide. Distortion of several of the foil traces is readily seen. Although not apparent in this photo, many of the silicone rubber spans intended to keep the electrode alignment in place have torn as well.

Step 4: Lamination to Make Spiral Cuff

After examining the prototype and removing it from between the slides, we proceeded with the final step in the fabrication, the lamination to make the spiral cuff. Our approach was to use only a single layer of stretched silicone rubber sheeting and a bottom coating of silicone rubber elastomer. The sheeting was 75μm in thickness, rather than the 50μm used in the first lamination step. Although we were unsure of the appropriate stretch to apply given the unknown stiffness of the PMP, we calculated the stretch according to our standard formula for a 3 mm diameter final cuff.

The PMP prototype was first cleaned using subsequent solutions of 10% Liquinox, filtered water, 95% ethanol, and ultrapure water, with a 5 minute sonication in each solution. A piece of 75μm silicone rubber sheeting was similarly cleaned. Both were allowed to airdry under a laminar flow bench. A layer of silicone rubber elastomer was spread on the bottom plate that had been treated with a mold release agent. The PMP prototype was laid on top of the elastomer and more elastomer was spread over the PMP, covering the entire structure. The stretched sheet was then placed over this sandwich.

A relatively large volume of elastomer had been used to ensure that plenty of elastomer was present to fill the voids in the PMP and to create the back side of the spiral cuff. In hindsight, using this much material was not beneficial. To flatten down to the final cuff thickness, the bulk of the material, located in the center and surrounding the foil, was forced to the periphery and had to flow past and through the cuts in the prototype. In those areas where the silicone rubber islands had torn during removal from the glass slide, this mass of material being forced out acted to further separate the pieces, and in fact, tear more of them.

This was particularly evident when the plates were opened and the final cuff was revealed. Multiple regions were separated and seen to bend away from one another. Upon close examination, it appears that the design performed exactly as intended by providing controlled stress relief without failure of the platinum foil pathway. Although the electrode did separate to some degree, this can primarily be attributed to the problems with adhesion to the glass slide. In those areas where the silicone rubber did not tear during removal, the structure held together.

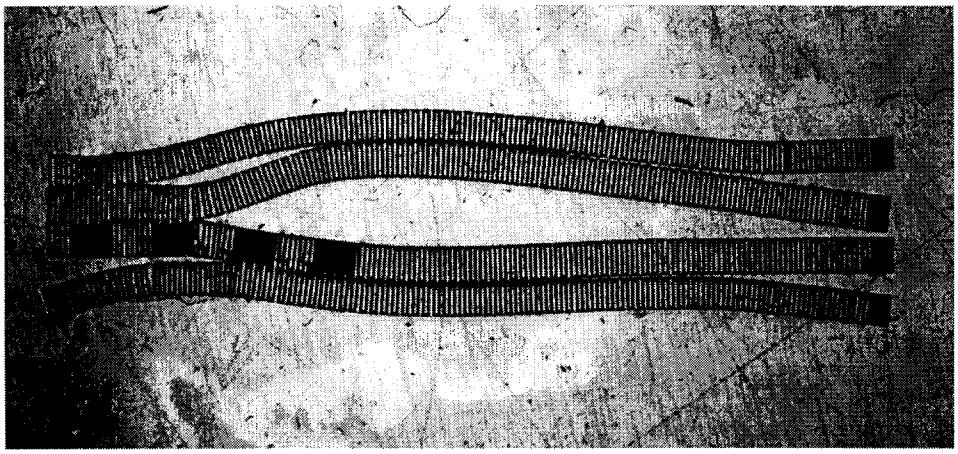

Figure 18: Photograph of PMP prototype after the final lamination. The electrode substrate separated in several areas. These areas were limited to regions were the silicone rubber had been torn prior to the final lamination step.

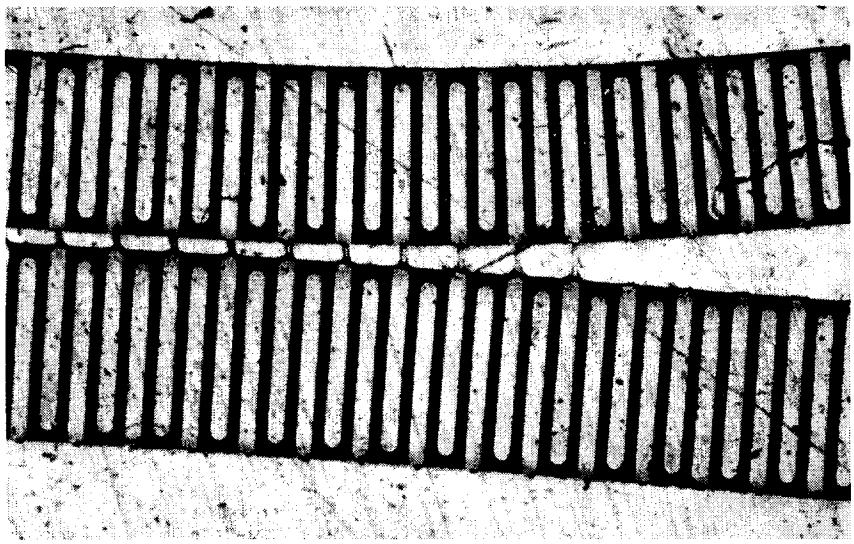

Figure 19: Photograph at higher magnification of a region of the PMP prototype cuff. The silicone rubber spans between the two 'rows' of tracings can be seen both stretched and broken. This allowed the overall structure to become misaligned. However, the metal tracings accommodate the stress and no breakage of the foil can be seen.

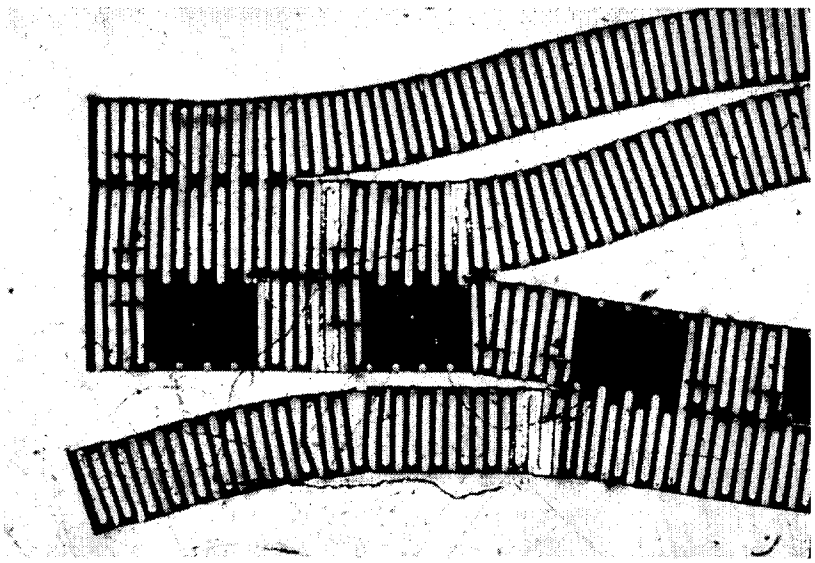

Figure 20: Photograph of the contact end of the PMP prototype cuff. In this region, much distortion was present before the final lamination process. Additional distortion was created during the final lamination, but the foil can be seen to accommodate this without breakage. Regions where the silicone rubber had not been torn are intact and properly aligned.

The resulting cuff is very flexible and no distortion in the curl or shape of the cuff is seen. The final diameter is slightly increased from nominal, which is not unexpected. However, if the cuff is forced to a smaller diameter by intentional rolling of the cuff, the PMP electrode accommodates this with minimal additional resistance and no apparent distortion in curl. The flexibility of the cuff can be further demonstrated by stretching it in the longitudinal direction. If the cuff is unrolled and tension applied at either end, the stress relief and flexion of the foil legs can be seen with the naked eye. Release of the tension results in the foil legs returning to their parallel alignment, with no visible breakage.

Future Work

To make a functional cuff, additional fabrication steps are necessary. These include exposing the platinum foil at the sites for lead wire connection and at the sites for the contacts. While these steps may be feasible to perform with the laser, we have opted to do them in-house for this prototype. Once the platinum foil has been exposed in the appropriate sites, the electrode can be tested for electrical continuity and isolation of each pathway. Our intention is to spot weld the lead wires to the bonding pads. We anticipate that a special welding pin configuration will have to be assembled so that the welding electrodes can make good contact with the foil, which is recessed within the silicone rubber lamination.

Although the fabrication to this point has not been without complications, we feel that the concept of the PMP has been verified. We will explore altering the dimensions and spacing of electrode components in an attempt to improve the reliability and strength of the electrode assembly. Some features of the FWF electrode design may be integrated with the revised PMP. Our efforts will continue with the 50μm foil, as the flexibility of the substrate does not appear to be a limitation.

SECTION C. IN VIVO EVALUATION OF ELECTRODES

C.I.2.1.2: Electrode Selectivity: Adjacent and Separate Fascicles

Abstract

Applying field steering techniques to electrodes implanted on the cat sciatic nerve, we have found it possible to effect selective activation of adjacent fascicles within the nerve trunk. These fascicles were not previously accessible to independent activation using short duration cathodic stimuli applied through a single contact of the four contact self-sizing cuff electrode. These results were demonstrated in five animals. In four of the studies, field steering applied at a constant 90% of the amplitude for threshold was found to be adequate to divert the excitatory field to an adjacent fascicle which was previously inaccessible to independent activation. In the fifth study, field steering was varied over a range of values to demonstrate our capacity to effect a graded degree of selectivity. Specifically, these results have demonstrated that it is possible, using a four contact self-sizing cuff electrode, to effect controlled and selective activation of any of the four fascicles contained in the sciatic nerve of a cat. Generally, these results are consistent with the hypothesis that multi-contact self-sizing cuff electrodes can be used to effect selective and controlled electrical activation of separate fascicles in a nerve trunk serving multiple muscles.

Purpose

The purpose of this project is to demonstrate selective activation, from threshold to maximum, of any specific motor nerve contained within a major nerve serving several muscles. The model system studied uses a four contact self-sizing cuff electrode placed on the cat sciatic nerve, which contains four major branches that serve the 13 muscles controlling the torque produced about the ankle. The focus of the studies reported here was to demonstrate that either of two adjacent fasciculi, serving separate muscles, but which cannot be separately activated using conventional stimulation techniques, can be activated separately and independently with "field steering" techniques.

Progress

Data were recorded and processed from five experiments during this reporting period. The methods used are described by Grill et al.(1996). Briefly, self-sizing spiral cuff electrodes were placed on the sciatic nerve of adult cats and the ankle torque was measured in response to electrical stimuli applied to the radially spaced contacts in the cuff. The focus of our efforts during this period was to demonstrate that field steering techniques can be used to activate selectively and controllably those fascicles that could not be activated individually through stimuli applied to a single contact. In these experiments, we intended to first identify a fascicle that could not be isolated when stimuli were applied to a single contact. We then proceeded to show that the excitatory field could be shifted away from or toward the particular fascicle in a controlled manner by the application of "steering" currents (anodic or cathodic respectively) to adjacent or opposite contacts on the radially spaced array.

Experiment #1: Cat #262

In Figure C.1 is shown the torque evoked around the ankle joint in Cat #262. The upper panel provides a post mortem representation of the electrode contact position relative to the four motor fascicles of the sciatic nerve. In this animal, we intended to generate selective activation of the common peroneal branch of the sciatic nerve. The lightly grayed data were recorded when stimuli were applied to the four main motor nerve branches of the sciatic nerve: the common peroneal (labeled **CP**), the tibial (labeled **Tib**), the lateral gastrocnemius/soleus (labeled **LG**) and the medial gastrocnemius (labeled **MG**). These data provide an indication of the magnitude and

direction of torques produced by the individual branches and presumably by the individual fascicles.

With stimulation applied to single contacts of the multi-contact spiral cuff, no torques were generated that could be closely correlated to activation of the common peroneal branch alone. Stimuli applied to the contact designated 180° produced a torque that was characteristic of the tibial nerve branch or some combination of tibial and common peroneal (designated **m181 and m182**). The simultaneous application of cathodic stimuli of varying amplitudes to contact 180° and an anodic stimulus applied between contact 90° and returned through contact 180°, at a constant value that was 90% of threshold, produced a torque that was consistent with selective activation of the common peroneal fascicle (designated **m18s091**, **m18s0911** and **m18s092** for three separate runs). The simultaneous application of cathodic stimuli of varying amplitudes to contact 180° and an anodic stimulus applied between contact 0° and returned through contact 180°, at a constant value that was 90% of threshold, produced some evidence of steering toward the common peroneal branch but did not produce a torque that was consistent with selective activation of the common peroneal fascicle (designated **m18s001** and **m18s002** for two separate runs). These results support the hypothesis that a positive steering current can shift the excitatory field away from a particular electrode to favor activation of a region closest to the contact where the cathodic stimulus was applied.

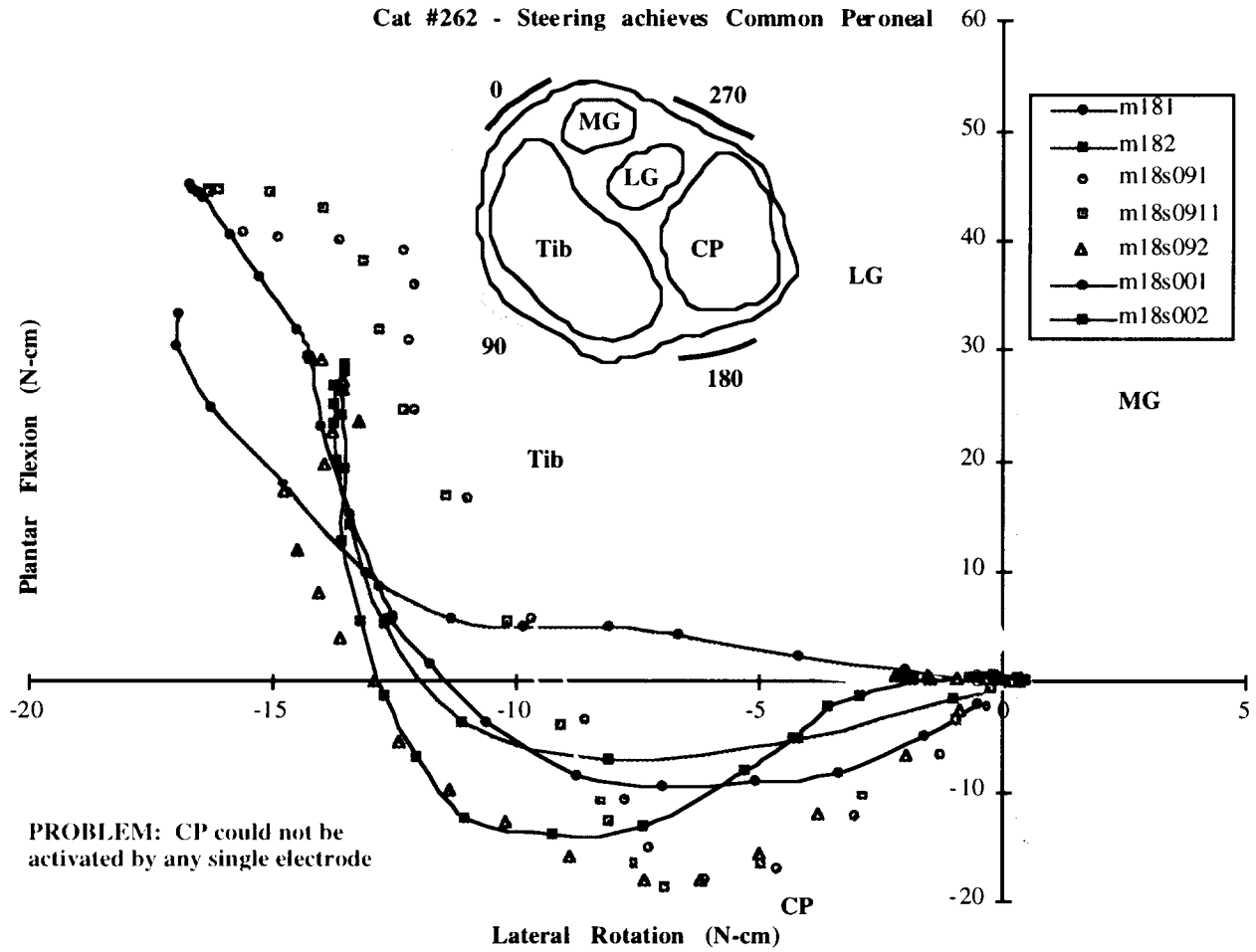

Figure C.1: The torque output of Cat #262 showing how the excitatory field produced from the 180° contact shifts to excite the common peroneal due to the introduction of anodic field steering from the 90° contact.

Experiment #2: Cat #256 In Figure C.2 is shown the torque evoked around the ankle joint of Cat #256. The lower right panel is a post mortem representation of the electrode contact position relative to the four motor fascicles of the sciatic nerve. The lightly grayed data were recorded when stimuli were applied directly to the lateral gastrocnemius/soleus (labeled **LG/Sol**) and the medial gastrocnemius (labeled **MG**)branches of the sciatic nerve.

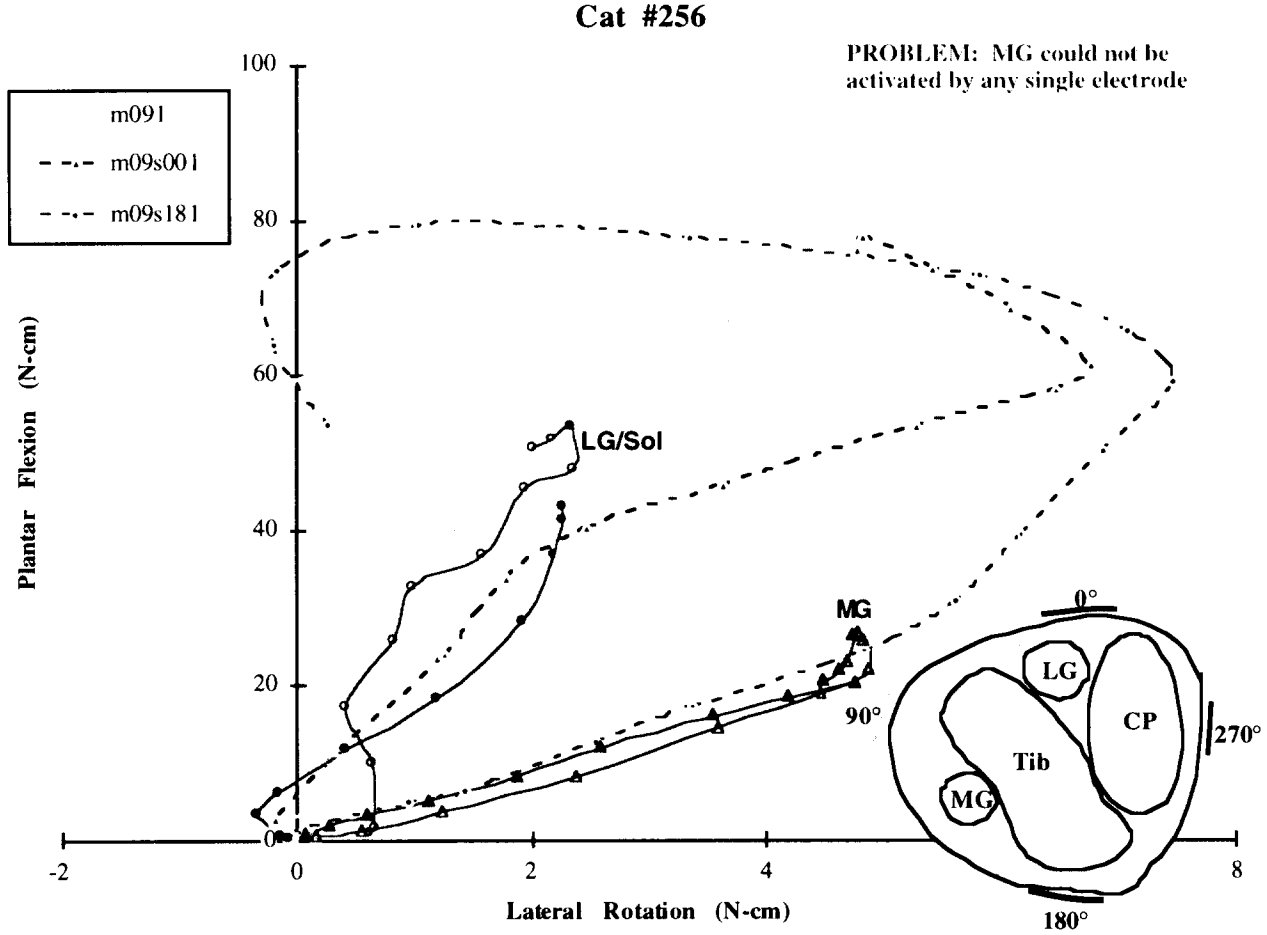

Figure C.2: The torque output of Cat #256 showing how the excitatory field produced from the 90° contact shifts to excite the medial gastrocnemius or the lateral gastrocnemius and soleus due to the introduction of anodic field steering from the 180° and the 0° contacts respectively.

In this animal, selective activation of the medial gastrocnemius branch could not be generated using conventional stimulation techniques. Stimuli applied to the contact designated 90° produced a torque that was characteristic of some combination of the medial gastrocnemius and lateral gastrocnemius/soleus branches (designated **m091**). The simultaneous application of cathodic stimuli of varying amplitudes to contact 90° and an anodic stimulus applied between contact 0° and returned through contact 90°, at a constant value that was 90% of threshold, produced a torque that was consistent with selective activation of the lateral gastrocnemius/soleus branch (designated **m09s001**). The simultaneous application of cathodic stimuli of varying amplitudes to contact 90° and an anodic stimulus applied between contact 180° and returned through contact 90°, at a constant value that was 90% of threshold, produced a torque that was consistent with selective activation of the medial gastrocnemius branch (designated **m09s181**). In both cases where steering currents were applied, the shift in excitability appears to be toward the

steering anode rather than away from the steering anode. These results are in conflict with the hypothesis that a positive steering current shifts the excitatory field away from a particular electrode to favor activation of a region closest to the contact where the cathodic stimulus is applied. Although our understanding of field steering is incomplete, a likely explanation for these conflicting results is the inadvertent reversal of polarity of the steering currents when the current generators were connected to the electrodes.

Experiment #3: Cat #244

In Figure C.3 is shown the torque evoked around the ankle joint of Cat #244. The lower right panel is a post mortem representation of the electrode contact position relative to the four motor fascicles of the sciatic nerve. Again, the lightly grayed data were recorded when stimuli were applied directly to the four main motor nerve branches of the sciatic nerve: the common peroneal (labeled **CP**), the tibial (labeled **Tib**), the lateral gastrocnemius/soleus (labeled **LG**) and the medial gastrocnemius (labeled **MG**).

In this experiment, selective activation of either the lateral gastrocnemius/soleus fascicle or of the medial gastrocnemius fascicle could not be achieved using stimuli applied from the 270° position contact only. Stimuli applied to that 270° contact produced a torque that was characteristic of some combination of the medial gastrocnemius and lateral gastrocnemius/soleus branches (designated **271**). The simultaneous application of cathodic stimuli of varying amplitudes to contact 270° and an anodic stimulus applied between contact 0° and returned through contact 270°, at a constant value that was 90% of threshold, produced a torque that was consistent with selective activation of some combination of the tibial and either the lateral or medial gastrocnemius branches (designated **270s00**). The simultaneous application of cathodic stimuli of varying amplitudes to contact 270° and an anodic stimulus applied between contact 180° and returned through contact 270°, at a constant value that was 90% of threshold, produced a torque that was consistent with selective activation of the lateral gastrocnemius and soleus branch (designated **270s180**). The simultaneous application of cathodic stimuli of varying amplitudes to contact 270° and an anodic stimulus applied between contact 90° and returned through contact 270°, at a constant value that was 90% of threshold, produced a torque that was consistent with selective activation of the common peroneal branch (designated **270s90**). In each case where steering currents were applied, the shift in excitability appears to be toward the steering anode rather than away from the steering anode. While this result is in conflict with our expectations, it is consistent with the results of Cat #256. Again, it seems likely that a mistake in the polarity connections may be responsible. Despite the error in the polarity connections, the application of field steering current was able to produce selective activation of the lateral gastrocnemius/soleus branch. We were not able to produce selective activation of the medial gastrocnemius branch.

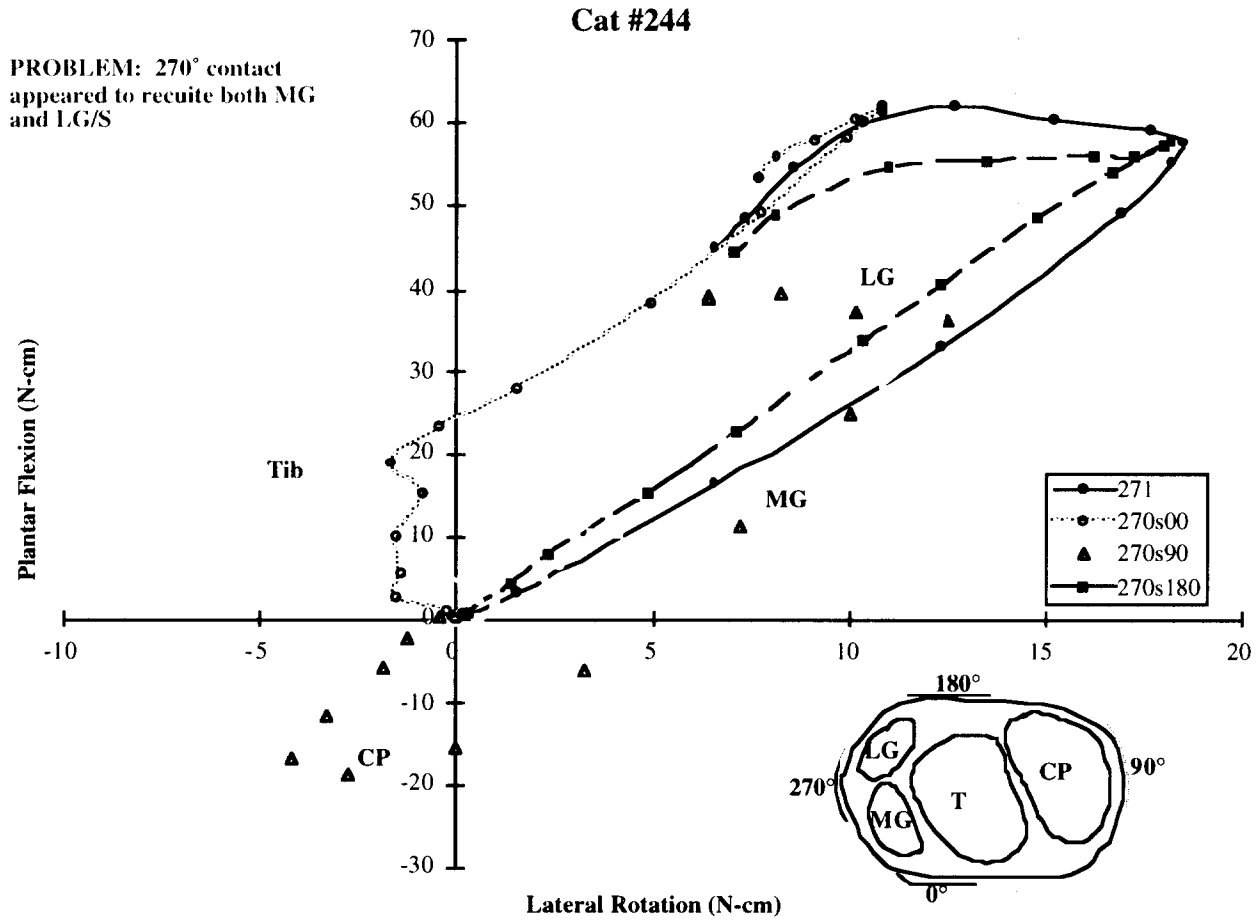

Figure C.3: The torque output of Cat #244 showing how the excitatory field produced from the 270° contact changes due to the introduction of anodic field steering from each of the other contacts around the equally spaced array.

Experiment #4: Cat #300

In Figure C.4 is shown the torque evoked around the ankle joint of Cat #300. Panels A, B and C provide a post mortem representation of the electrode contact position relative to the four motor fascicles of the sciatic nerve. The lightly grayed data were recorded when stimuli were applied to the four main motor nerve branches of the sciatic nerve, the common peroneal (labeled **CP**), the tibial (labeled **Tib**), the lateral gastrocnemius/soleus (labeled **LG**) and the medial gastrocnemius (labeled **MG**).

Stimulation applied to single contacts was unable to produce torques consistent with selective activation of the medial gastrocnemius branch. Stimuli applied to the contact designated 270° produced a torque that was characteristic of the lateral gastrocnemius/soleus branches (designated **270°**). The simultaneous application of independent cathodic stimuli of varying but equal amplitudes to contact 270° and contact 0° (as illustrated in panel A), produced a torque that was consistent with selective activation of the medial gastrocnemius branch (designated **m0027_0830** and **m0027_1245**). The simultaneous application of cathodic stimuli of varying amplitudes to both contact 270° and contact 0° together (as illustrated in panel B), produced a torque that was not highly consistent with selective activation of the medial gastrocnemius branch (designated **m0027x1520**). The simultaneous application of cathodic stimuli of varying amplitudes to both contact 270° and contact 0° together, and an anodic stimulus applied between both contact 90° and contact 180° and returned through both contact 270° and contact 0°, at a constant value that was 90% of threshold (as illustrated in panel C), produced a torque that was consistent with selective activation of the medial gastrocnemius branch (designated

m0027s0918_1250). In each case where steering currents were applied, the shift in excitability appears to be toward the steering anode rather than away from the steering anode. These results support the hypothesis that a negative steering current can shift the excitatory field towards a particular electrode to favor activation of a region closest to the contact where the cathodic stimulus was applied. These results also suggest that the application of a stimulus to two different contacts using a single current generator does not produce the same results as the application of current at equal levels of stimulation through 2 independent current generators attached to the same two contacts. The results of grouped stimulation was improved by the addition of anodic steering currents applied from the other two contacts.

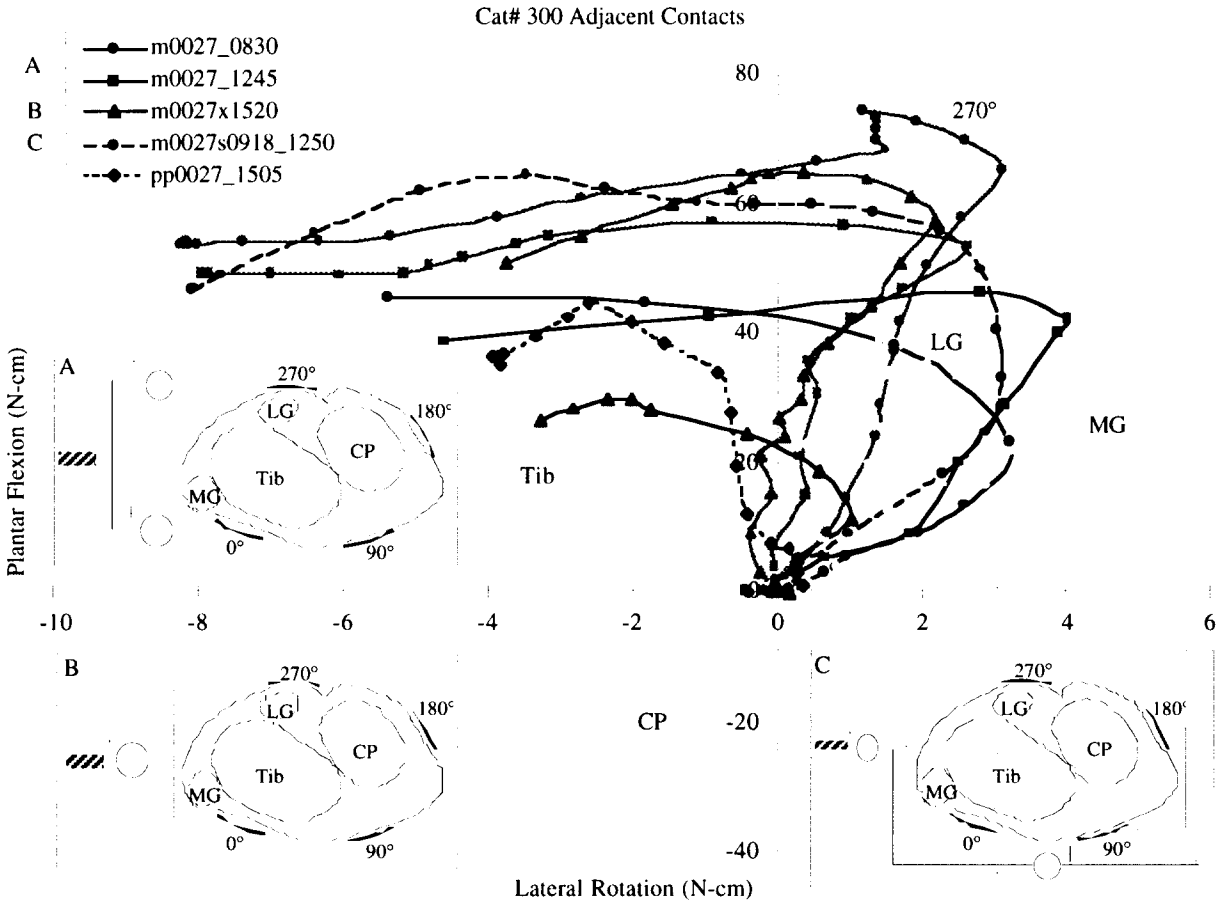

Figure C.4: The torque output of Cat #300 showing how the excitatory field produced from the 270° contact can be shifted to activate the medial gastrocnemius through the introduction of cathodic field steering from the 0° contact.

Experiment #5: Cat #302

In Figure C.5 is shown the torque evoked around the ankle joint of Cat #302. The lightly grayed data were recorded when stimuli were applied to the common peroneal (labeled **CP**) and the tibial (labeled **Tib**) branches of the sciatic nerve.

In this animal, selective activation of the common peroneal fascicle could not be produced using stimuli applied through a single contact at any position. Stimuli applied to the contact designated 270° produced a torque that was characteristic of some combination of the tibial and common peroneal branches (designated **270°**). We attempted to use steering currents to smoothly and gradually change the excitatory field of the 270° contact to activate selectively the common peroneal branch. The simultaneous application of cathodic stimuli of varying amplitudes to contact

270° and an anodic stimulus applied between contact 180° and returned through contact 270°, produced a range of torque that encompassed the region of torque space between the torque output produced by activation of the 270° contact alone and that produced by the common peroneal branch alone. The red color indicates higher levels of cathodic current applied to the 270° contact relative to the distant return and lower levels of anodic current applied to the 180° contact relative to the 270° contact. The yellow color indicates lower levels of cathodic current applied to the 270° contact relative to the distant return and higher levels of anodic current applied to the 180° contact relative to the 270° contact. These results support the hypothesis that a positive steering current can shift the excitatory field towards a particular electrode to favor activation of a region closest to the contact where the cathodic stimulus was applied. These results also suggest that the application of the positive steering current acts in a progressive and continuous manner to produce a gradual shift of the excitatory field.

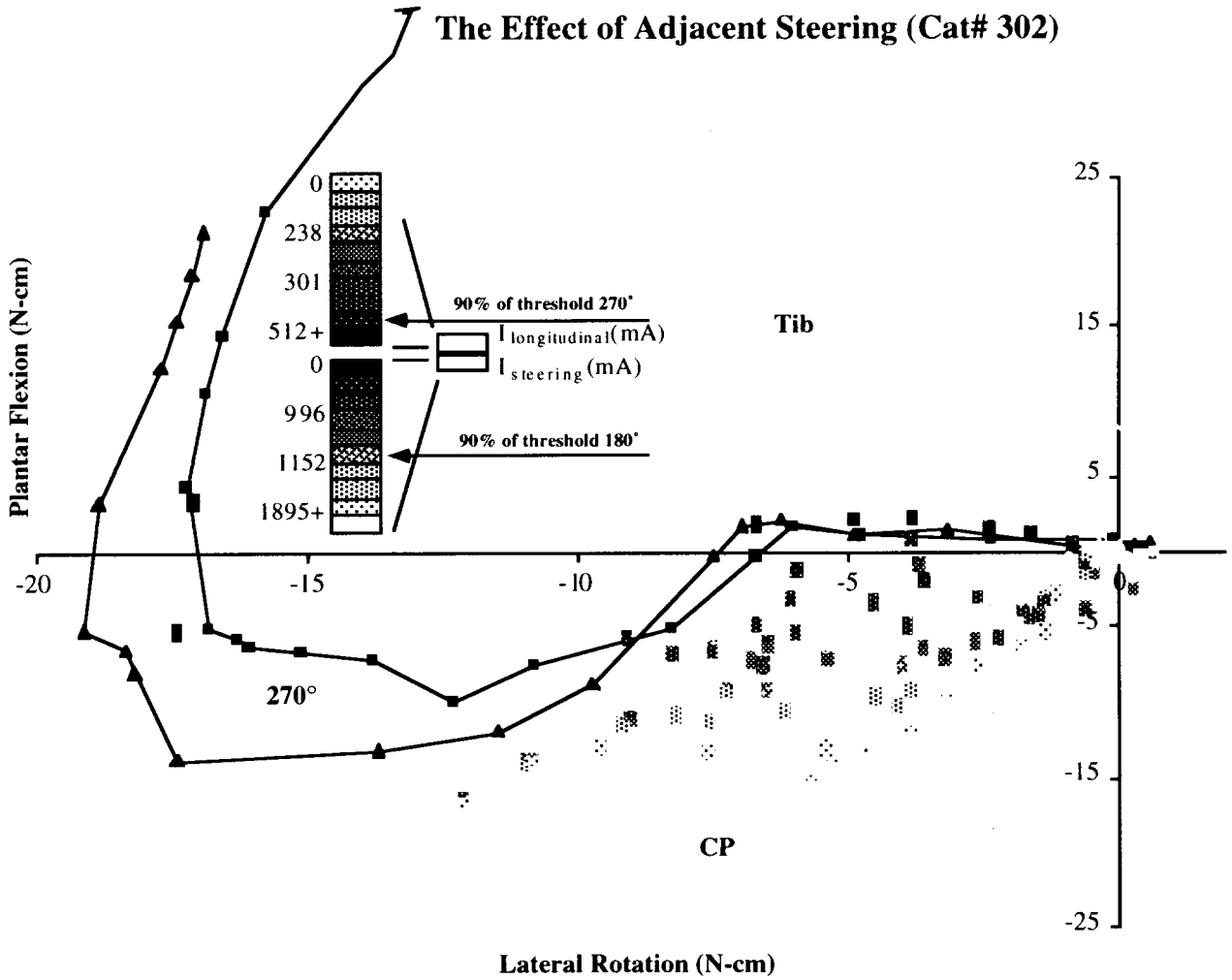

Figure C.5: The torque output of Cat #302 showing a graded and continuous shift of the excitatory field produced from the 270° contact as the amplitude of the anodic steering current from the 180° contact is increased until full common peroneal is achieved.

Conclusion

Applying field steering techniques to electrodes implanted on the cat sciatic nerve, we have found it possible to effect selective activation of fascicles that were not previously accessible to electrical activation using short duration cathodic stimuli applied to a single contact of a four contact self-sizing cuff electrode. These experiments support the hypothesis that with a multi-contact, self-

sizing, spiral cuff electrode, it is possible to activate selectively, from threshold to maximum activation, any specific motor nerve contained within a major nerve serving several muscles. Additionally, we found it possible to gradually and smoothly modulate the excitatory field to move the excitation from one fascicle to a different fascicle. In some cases, the fascicle activated due to the addition of steering currents did not correspond to the present hypothesis of how the steering current works. Two possible explanations were proposed for these situations including inadvertent experimental error and incomplete understanding of field steering. In all cases, however, we found it possible to fully activate a fascicle when it was not previously possible to activate and we found it possible to activate a single fascicle from a contact that previously activated multiple fascicles together.

Reference

Grill, W.M., and J.T. Mortimer. "Non-invasive measurement of the input output properties of peripheral nerve stimulating electrodes." J Neurosci Methods, 65:43-50 (1996).